ORIGINAL PAPER

Effects of Single and Double Bonds in Linkers on Colorimetric and Fluorescent Sensing Properties of Polyving Akohol Grafting Rhodamine Hydrazides

Tong-Mou Geng · Xie Wang · Zhu-Qing Wang · Tai-Jie Chen · Hai Zhu · Yu Wang

Abstract Two rhodamine derivatives, N-mono-maleic acid amide-N′-rhodamine B hydrazide (MRBH) and N-mono-succinic acid amide-N′-rhodamine 6G hydrazide (SR6GH), were synthesized by amidation with maleic anhydride (MAH), succinic anhydride (SAH) and rhodamine B hydrazide, rhodamine 6G hydrazide, which were identified by FTIR, ^{1}H NMR and elemental analysis. Two water-soluble fluorescent materials (PVA-MRBH and PVA-SR6GH) were prepared via esterification reaction with N-mono-maleic acyl chloride amide-N′-rhodamine B hydrazide (MRBHCl) or N-mono-maleic acyl chloride amide-N′-rhodamine 6G hydrazide (SR6GHCl) and poly(vinyl alcohol) (PVA) in DMSO solution. The sensing behaviors of PVA-MRBH and PVA-SR6GH were explored by recording the fluorescence spectra in completely aqueous solution. Upon the addition of Cu^{2+} and Fe^{3+} ions to the aqueous solution of PVA-MRBH, visual color change from rose pink to amaranth and orange for Cu^{2+} and Fe^{3+} ions, respectively, and fluorescence quenching were observed. Titration of Cu^{2+}, Fe^{3+}, Cr^{3+} or Hg^{2+} into the aqueous solution of PVA-SR6GH, although they induced

fluorescence enhancement, only Fe^{3+} made the color changing from colorless to yellow. Moreover, other metal ions did not induce obvious changes to color and the fluorescence spectra.

Introduction

Development of chemosensors for sensing and recognition of environmentally and biologically important heavy and transition metal ions, for example, Hg^{2+}, Cu^{2+}, Fe^{3+} and Cr^{3+}, have attracted considerable attention of current researchers [1–9]. Fluorescent chemosensors provide several advantages over other analytical methods, such as high sensitivity, specificity, convenience, real time monitoring with fast response times, and low cost [10]. During the past decades, increasing research interests have been devoted to the fluorescence sensing of heavy and transition metal ions [11].

Because rhodamine dyes have many advantages such as low cost, long-wave length absorption/emission, high molar absorption coefficient, high quantum yield, and photostability [12–15]. They have been widely used as a molecular platform for the design of new spectroscopic probes [3, 10]. Moreover, in the absence of cations, these rhodamine-based chemosensors exist in a spirocyclic form, which is colorless and non-fluorescent. The addition of a specific metal ion leads to spirocycle unit opening via coordination or irreversible chemical reaction, resulting in the appearance of a pink color

T.-M. Geng (✉) · X. Wang · Z.-Q. Wang · T.-J. Chen · H. Zhu
Anhui Key Laboratory of Functional Coordination Compounds,
School of Chemistry and Chemical Engineering, Anqing Normal
University, Anqing 246011, People's Republic of China
e-mail: gengtongmou@aqtc.edu.cn

Y. Wang
School of Resource and Environmental Science, Anqing Normal
University, Anqing 246011, People's Republic of China

or orange fluorescence [3, 6, 15]. Thereby, the rhodamine fluorophore can be an ideal framework to construct off–on system for the specific metal ion [8]. Exploiting this idea in 1997, Czarnik et al. first reported rhodamine based chemosensor [16]. Following this work, the spirolactam-ring opening phenomenon has been utilized by many groups and a number of reports have appeared in literature for the detection of various ions based on rhodamine as signalling moiety [4, 8, 12, 17].

Up to now, variety of chemosensors for metal ions have been fabricated from small organic molecules based rhodamine derivataves [3]. However, most of these small molecular chemosensors typically exhibit poor water solubility, which partially limits their practical applications in diverse fields [4, 11]. This inconvenience can be overcome by using hydrophilic copolymers that also contain small amounts of the lipophilic organic

receptors [18]. At present, there are some fluorescent polymeric sensors with different macromolecular structure for the detection of metal cations and protons in the environment [19–23].

Earlier we have developed polymeric sensors based on rhodamine in "off-on" mode for the detection of metal cations in aqueous solution [24–26]. As part of our continuous work on polymeric chemosensors based on polyving akohol grafting the rhodamine derivative [24], we prepared severally two water-soluble polymers, polyving akohol grafting N-mono-maleic acid amide-N′-rhodamine B hydrazide (PVA-MRBH) and polyving akohol grafting N-mono-succinic acid amide-N′-rhodamine 6G hydrazide (PVA-SR6GH), (Scheme 1). Unexpectedly, we found that the derivatives display obvious differences in fluorescence sensory pattern, metal cation species and color changes.
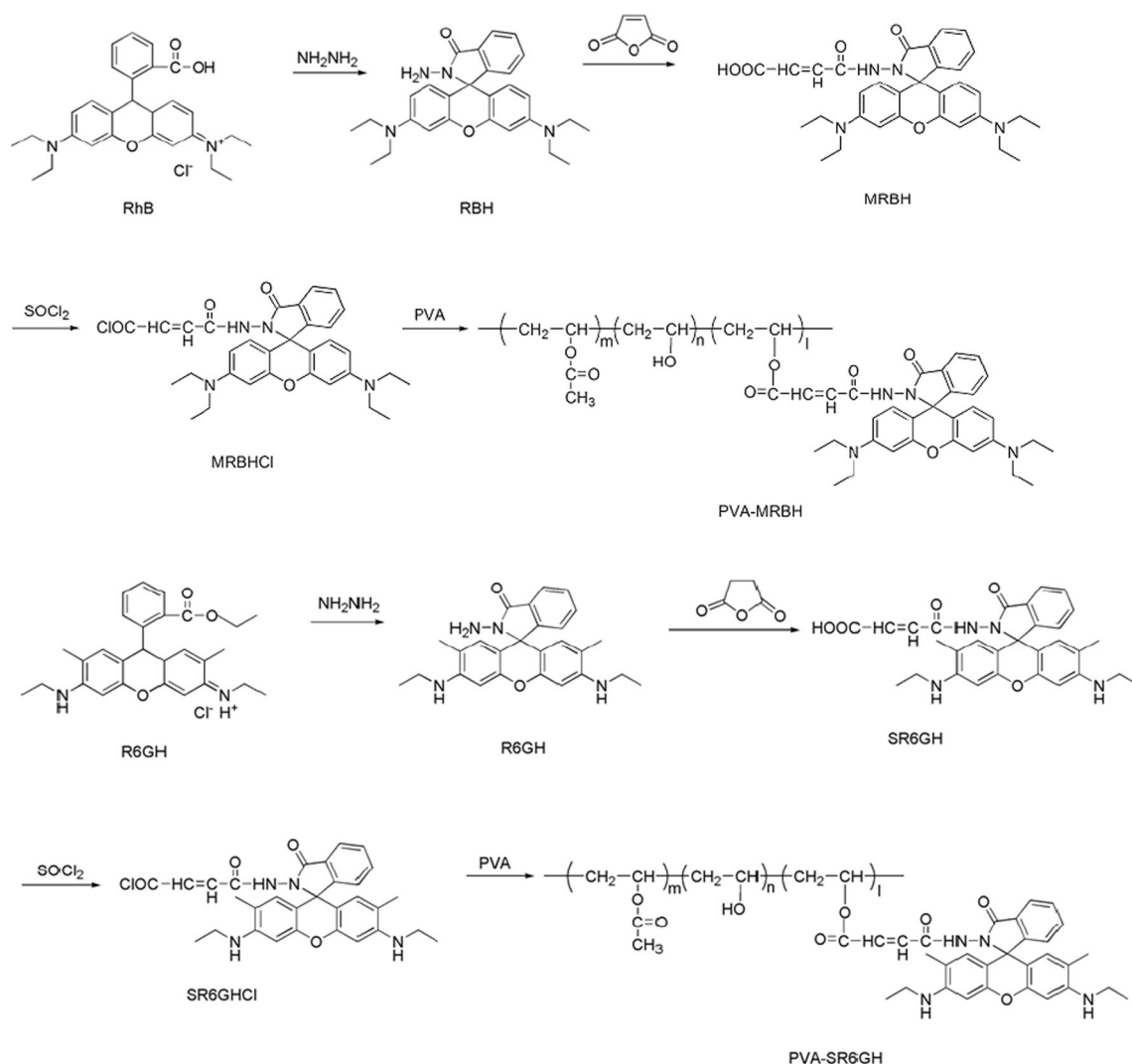
Scheme 1 Synthesis of MRBH, SR6GH, PVA-MRBH and PVA-SR6GH

Experimental

As shown in Scheme 1, rhodamine containing copolymers PVA-MRBH and PVA-SR6GH were easily obtained by using postfunctionalization strategy. Firstly, the acylation reaction of maleic anhydride (MAH) with rhodamine B hydrazide (RBH) or of succinic anhydride (SAH) with rhodamine 6G hydrazide (R6GH) were carried out [27–29]. Then, the rhodamine moieties were linked to polyving akohol by esterification reaction between MRBHCl or SR6GHCl and the -OH functional group of PVA after transforming to acyl chloride from carboxylic acid. Although increased one step reaction using the esterification by acyl chloride with –OH of PVA, the yield was raised [30, 31]. Polyving akohol (PVA) is a polymeric material available in the market, which has good solubility in water. It can be modified due to the presence of abundant OH functional groups in the backbone [30]. Rhodamine B and rhodamine 6G belong to homolog, they have analogous fluorescent property [13].

Materials

PVA (Anhui Wanwei updated High-tech material industry company limited, Hefei, China) used in this study had a degree of polymerization of 1700 with a saponification value of 99 % with an average molecular weight of 75 000, and dried at 40 °C for 24 h before use. Rhodamine B, rhodamine 6G, maleic anhydride (MAH) and succinic anhydride (SAH) were purchased from Sigma-Aldrich Trading Co. Ltd. (Shanghai, China); Hydrazine hydrate, thionyl chloride and dimethyl sulfoxide (DMSO) were purchased from Sinopharm Chemical Reagent Co. Ltd. (Shanghai, China) and used without further purification; Anhydrous methanol and ethanol, acetic ether, dichloromethane, petroleum ether, N,N-dimethylformamide (DMF) and pyridine were obtained from commercial suppliers. Rhodamine B hydrazide (RBH) and rhodamine 6G hydrazide (R6GH) were prepared according to the literature method [32–35].

Instrumentation

The ^{1}H NMR spectra were measured on a DRX 400 Bruker spectrometer (AVANCE AV 400, Bruker corporation, Switzerland) at 298 K in CDCl$_3$ or D$_2$O with TMS as internal standard. FTIR spectra were recorded on a Nicolet Neus 8700 FTIR spectrophotometer (Thermo Scientific Instrument Co. U.S.A) with KBr compressing tablet. Elemental analyses (C, H and N) were carried out on a VarioELIII analyzer (Elementar corporation, Germany) for MRBH and SR6GH. All pH measurements were made with a Model pHS-3C pH meter (Shanghai, China). Fluorescence spectra were acquired on a RF5301PC fluorescence spectrophotometer (Shimadzu Corporation, Japan).

Synthesis

Synthesis of N-Mono-Maleic Acid Amide-N′-Rhodamine B Hydrazide (MRBH) and N-Mono-Succinic Acid Amide-N′-Rhodamine 6G Hydrazide (SR6GH)

N-mono-maleic acid amide-N′-rhodamine B hydrazide (MRBH) were prepared according to literature protocol [3, 27, 28]. Briefly, rhodamine B hydrazide (RBH) (0.4566 g, 1.0 mmol) was dissolved in dichloromethane (30 mL), to which a solution of maleic anhydride (MAH) (0.1975 g, 1.0 mmol) in dichloromethane (10 mL) was added dropwise. The resulting solution was stirred at 50 °C for 4 h, and then the solvent was removed under reduced pressure to get a violet-red residue, which was purified by silica-gel column chromatography with ethyl acetate-petroleum ether (bp 60–90 °C) (1:9, v/v) as eluent, affording 0.1956 g of MRBH (Yield: 42.77 %). FTIR of MRBH: 3508.46, 3441.66 (s, ν_{-NH2}); 2924.76 (s, ν_{-CH3}), 2850.16(s, ν_{-CH2}); 1700.31(s, $\nu_{c=o}$); 1630.29 (s, $\nu_{Ar\ C=C}$); 1573.04 (m, $\nu_{Ar\ C=C}$), 1463.32, 1382.13 (m, $\nu_{Ar\ C=C}$). ^{1}H NMR (400 MHz, CDCl$_3$, 298 K) of MRBH: 7.83 (d, Ar-H), 7.46 (m, C=C-H), 7.39 (d, Ar-H), 7.25 (d, Ar-H), 7.24(d, Ar-H), 6.97 (s, C=C-H), 6.84(d, Ar-H), 6.19 (d, Ar-H), 6.13 (d, Ar-H), 3.39 (n, −CH$_2$-), 1.13 (m, −CH$_3$). Elemental analysis, calcd. for C$_{32}$H$_{34}$N$_4$O$_5$: C 69.30, H 6.18, N 10.10 %; found, C 69.41, H 6.32, N 9.72 %.

The synthesis of N-mono-succinic acid amide-N′-rhodamine 6G hydrazide (SR6GH) was similar to MRBH (Yield: 37.0 %). FTIR of SR6GH: 3423.11 (s, ν_{-NH2}); 2973.04, 2931.28 (s, ν_{-CH3}), 2877.15(s, ν_{-CH2}); 1690.90(s, $\nu_{c=o}$); 1632.13 (s, $\nu_{Ar\ C=C}$); 1514.58 (m, $\nu_{Ar\ C=C}$), 1424.88, 1383.12 (m, $\nu_{Ar\ C=C}$). ^{1}H NMR (400 MHz, CDCl$_3$, 298 K) of SR6GH: 7.88–7.89 (d, Ar-H), 7.37–7.88 (m, Ar-H), 6.96–6.99 (d, Ar-H), 6.43 (s, Ar-H, −CO-NH-N), 6.21 (s, Ar-H), 3.63–3.68 (m, Ar-NH-CH$_2$-), 3.14–3.19 (m, Ar-NH-CH$_2$-), 2.55–2.59 (d, Ar-H), 6.13 (m, −CH$_2$–COOH), 3.39 (m, −CH$_2$-CO-NH-), 1.89(m, −CH$_2$),1.14–1.29 (m, −CH$_3$). Elemental analysis, calcd. for C$_{30}$H$_{32}$N$_4$O$_5$: C 68.17, H 6.10, N 10.60 %; found, C 68.21, H 6.22, N 9.98 %.

Synthesis of PVA-MRBH and PVA-SR6GH

Addition of 1 drop of N,N-dimethylformamide (DMF), 1 mL of dichloromethane, 0.5546 g (1 mmol) of MRBH, 0.18 mL of SOCl$_2$ (1.5 mmol) in three-necked flask of 100 mL, the mixture was magnetic stirred for 12 h at room temperature and then was reacted under reflux for 2 h. The residual SOCl$_2$ was removed by the reduced pressure distillation, affording pink solid of acyl chloride, N-mono-maleic acyl chloride amide-N′-rhodamine B hydrazide (MRBHCl) [28].

PVA solution in DMSO was prepared by adding 3.312 g of purified PVA powder to 50 mL of DMSO and heating this mixture to 80 °C with continuous mechanical stirring until a

clear solution was obtained. 0.2210 g (0.3856 mmol) of MRBHCl was dissolved in 5 mL dimethyl sulfoxide (DMSO) and added the solution to PVA solution of DMSO by dropping funnel under agitating at 80 °C. The mixture was reacted in an oil bath at 80 °C by mechanical stirring for 5 h. While cooled to room temperature, the orange solution was allowed to precipitate in excess anhydrous methanol to provide a pink deposit. After vacuum filtration, the solid was washed with ethanol until the solvent was not fluorescent. The powder was then put in a Soxhlet extractor and extracted with ethanol and chloroform for at least 12 h, respectively, to ensure that there was noncovalently bounded RBH or MRBH in PVA. The desired product was ultimately synthesized via vacuum drying (Yield: 83.51 %), as illustrated in Scheme 1. [20, 36]. FTIR of PVA-MRBH (KBr), cm^{-1}: 3444.83(ν $_{PVA-OH}$); 2909.05–2951.1, 2843.57($\nu_{-CH2-,-CH-}$); 1645.45($\nu_{C=O}$); 1469.91, 1329.47, 1232.92, 1145.14($\nu_{aromatic C=C}$); 1099.06(ν_{C-O}); 1423.82 (δ_{C-H}). ^{1}H NMR (400 MHz, D$_2$O, 298 K) of PVA-MRBH: 7.94 (d, Ar-H), 7.46 (d, C=C-H), 7.31 (m, CO-NH-), 7.24 (d, Ar-H), 7.2–7.1 (d, Ar-H), 6.97, 6.90 (d, C=C-H, Ar-H), 6.19 (s, Ar-H), 6.13 (d, Ar-H), 4.65, 4.52, 4.45 (d, −OH), 4.51 (d, −C$\underline{H}$-MRBH), 3.89 (m, −C$\underline{H}$-OOCCH$_3$), 3.41 (m, −OOCCH$_3$), 3.32 (d, −C$\underline{H}$-OH), 2.51, 2.50, 2.498 (m, −C$\underline{H}_2$-CH$_3$), 1.59–1.37 (m, −CH$_2$-), 1.07, 1.06, 1.04 (m, −CH$_2$-C$\underline{H}_3$).

The preparation of PVA-SR6GH was similar to PVA-MRBH (Yield: 87.27 %). FTIR of PVA-SR6GH (KBr), cm^{-1}: 3444.76 (ν $_{PVA-OH}$); 2920.46, 2846.32 ($\nu_{-CH2-,-CH-}$); 1632.13 ($\nu_{C=O}$); 1462.00, 1387.46, 1134.11 ($\nu_{aromatic C=C}$); 1099.00 (ν_{C-O}); 1414.05 (δ_{C-H}). ^{1}H NMR (400 MHz, D$_2$O, 298 K) of PVA- SR6GH: 1.04–1.08 (m, −CH$_2$-C$\underline{H}_3$), 1.60–1.38 (m, −CH$_2$-), 1.99 (s, −Φ-CH$_3$), 2.50, (m, −CH$_2$-), 3.18 (s, CH$_3$CH$_2$-N$\underline{H}$-Φ), 3.32 (d, −C$\underline{H}$-OH), 3.41 (m, −OOCCH$_3$), −C$\underline{H}$-OOCCH$_3$), 4.66, 4.53, 4.46 (d, −OH), 6.31 (s,−Φ-H), 6.53–6.59 (s,−Φ-H), 7.07–7.10 (s,−Φ-H), 7.29 (s,−Φ-H), 7.30 (m, CO-NH-), 7.46–7.51 (s,−Φ-H), 7.97–8.01 (s,−Φ-H).

Preparation and Fluorescence Intensity of PVA-MRBH and PVA-SR6GH Aqueous Solution

PVA-MRBH and PVA-SR6GH, like PVA, were hard to dissolve in water at room temperature, so the polymer solutions of desired concentration were prepared by dissolving a known amount of PVA-MRBH or PVA-SR6GH in deionized water with gentle stirring at 80 °C, and were kept for 2 h to ensure homogenization [29]. For fluorescence emission measurements, a 10×10 mm quartz cell was used for detection. The effect of the metal cations on fluorescence intensity was examined by adding a few microlitre of stock solution of the metal cations to a known volume of the polymer solution (2.00 mL). The addition was limited to 0.10 mL, so that the dilution of the polymer solution remained insignificant [37]. The excitation and the emission slit widths were 10 nm and

5 nm, respectively, excitation wavelength was 500 nm, scanning range were from 520 to 650 nm, scanning speed was medium, and testing temperature was at 25 °C.

The detection limit was calculated with the equation: detection limit$=3S/\rho$, where S is the standard deviation of blank measurements and ρ is the slope between relative intensity versus sample concentration [18, 30].

Results and Discussion

Effect of Polymer Concentration on Fluorescence Intensity

Figure 1 was fluorescent emission spectra of PVA-MRBH in different polymer concentration under neutral conditions (λex=500 nm). Inset was effect of polymer concentration on fluorescence intensity. It can be seen that the higher the polymer concentration was, the stronger the fluorescence intensity was. Between fluorescence intensity (I) and polymer concentration ([P]) shown good line relationship ($R=0.9855$).

$$I = 3.329 + 6.176[P] \tag{1}$$

This indicated that rhodamine derivatives underwent equilibrium between spirocyclic (nonfluorescence) and ring opened (fluorescence) forms in the aqueous solution. Under certain pH, the contents of either the ring-opened or ring closed structures were increased with the increasing of polymer concentration [12, 38].

Time-Dependence of PVA-MRBH–Cu^{2+} Complex

The reaction between PVA-MRBH and Cu^{2+} ions was found to be instantaneous due to the presence of active phenyl hydrazide group but for time taken for complete reaction, which was studied by keeping all other reaction parameters constant. In a standard cuvette, 5 μL of 0.1 mol/L Cu^{2+} solution was added to 2 mL of 8.5 mg/mL PVA-MRBH ([Cu^{2+}]=2.5× 10^{-4} mol/L) and the fluorescence emission (λex=500 nm) values were measured and plotted as function of time [39]. As shown in Fig. 2, the time dependence of the response of PVA-MRBH to Cu^{2+} ions was investigated. It could be seen that the fluorescence signal of the PVA-MRBH with Cu^{2+} ion remarkably decreased for a few minutes, and leveled off as the time continues. The fluorescence intensity of PVA-MRBH with Cu^{2+} reached its minimum value at about 10 min, after which the fluorescence intensity remained almost constant [26, 40–44].

Fig. 1 Fluorescence emission spectra of PVA-MRBH in different polymer concentration (Inset Effect of polymer concentration on fluorescence intensity, λex=500 nm)
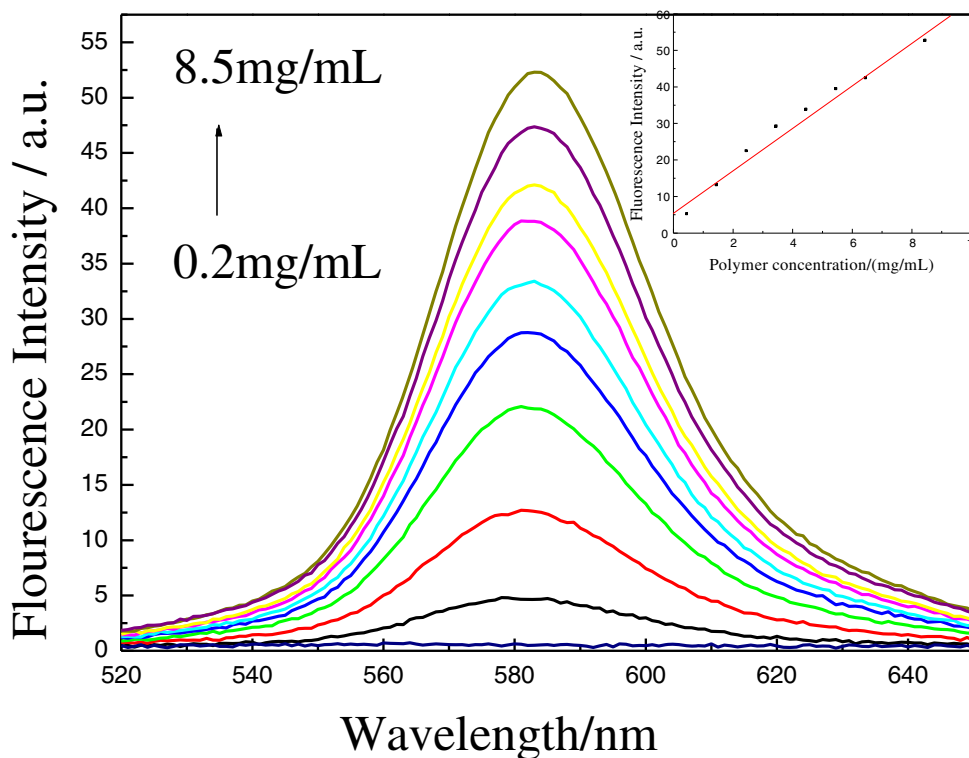
The Sensitivity of PVA-MRBH for Cu^{2+} and Fe^{3+}

The fluorogenic sensing behaviors of PVA-MRBH aqueous solutions were depicted in Fig. 3 (Cp=8.5 mg/mL, λex= 500 nm) [18]. Unlike most of the spirocycle RBH derivatives, when the polymer concentration was high, for example, 8.5 mg/mL, the aqueous solution of PVA-MRBH was rose pink and exhibited certain fluorescence property in neutral water, implying that there were a some of acid amides form. When the concentration of Cu^{2+} and Fe^{3+} added to the aqueous solution of PVA-MRBH were reached to 2.0×10^{-3} and 2.5×10^{-3} mol/L, the fluorescence was quenched and were reduced to a 0.58-fold and 0.60-fold, respectively (Fig. 3). The fluorescence turn-off were further supported by the observation that the emission color of the probe solution turned from pale pink to deep purple for Cu^{2+}, and from pale pink with orange red to orange for Fe^{3+}, respectively (Fig. 4) [22, 31, 44, 45].

Relative fluorescence intensities (I/I_0) at 583 nm obtained from Fig. S11 were plotted vs. Cu^{2+} or Fe^{3+} concentration and linear spectrofluoro-metric responses for Cu^{2+} or Fe^{3+}
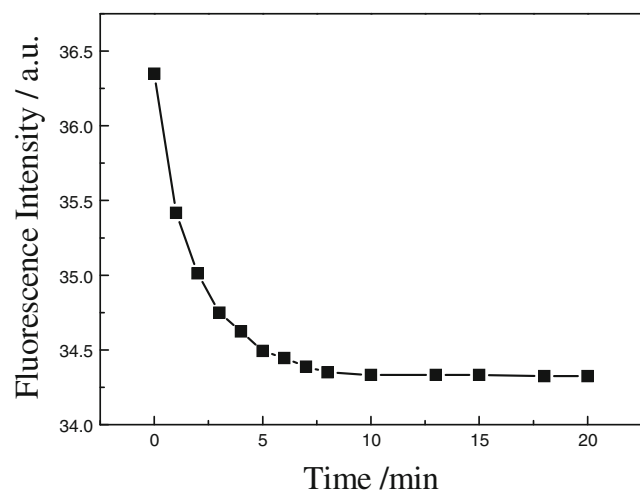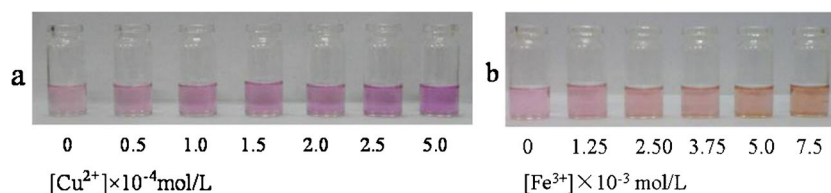

Fig. 2 Effect of time on fluorescence intensity of PVA-MRBH (Cp= 8.5 mg/mL, $[Cu^{2+}]=2.5 \times 10^{-4}$ mol/L, λex=500 nm)
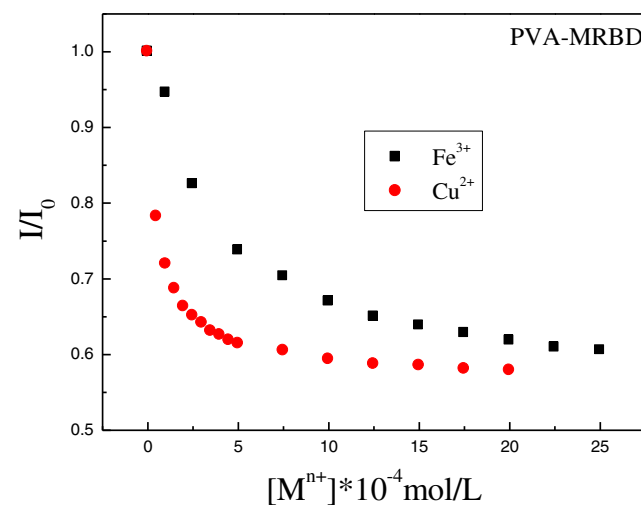
Fig. 3 The effect of Cu^{2+} or Fe^{3+} ions concentration ($[Cu^{2+}]$ or $[Fe^{3+}]$) on relative fluorescence intensity (I/I_0) of PVA-MRBH (Cp=8.5 mg/mL, λex=500 nm)

Fig. 4 Photographs recorded under visible light for aqueous solutions of PVA-MRBH (Cp=8.5 mg/mL) in the presence of different metal ions concentration ((a) $[Cu^{2+}]$=0–5.0×10^{-4} mol/L, (b) $[Fe^{3+}]$=0–7.50×10^{-3} mol/L)

concentration were obtained with very good regression coefficients as R=0.9740 and R=0.9834, respectively. These linear responses could be used for detection of Cu^{2+} or Fe^{3+} concentration using the following equations for concentration range between 0.5×10^{-4}–2.0×10^{-4} mol/L (a) and 0–5.0× 10^{-4} mol/L (b) (Eqs. 2 and 3, respectively):

$$I/I_0 = 0.8103 - 7.787 \times 10^2 \left[Cu^{2+}\right] \qquad (2)$$

$$I/I_0 = 0.9909 - 5.357 \times 10^2 \left[Fe^{3+}\right] \qquad (3)$$

where I is the emission intensity of tested sample at 583 nm and I_0 is the emission intensity of metal free polymer solution [31, 45, 46].

The detection limits, which were calculated as three times the standard deviation of the background noise from the calibration curve, for the determination of Cu^{2+} and Fe^{3+} ions in the same medium were found to be 3.85×10^{-6} and 8.40× 10^{-7} mol/L [18, 23, 31, 42].

The Sensitivity of PVA-SR6GH for Cu^{2+}, Fe^{3+}, Cr^{3+} or Hg^{2+}

Figure 5 presented the sensibility of the PVA-SR6GH (Cp= 1.0 mg/mL, λex=500 nm) in aqueous solution at different concentrations of Cu^{2+}, Fe^{3+}, Cr^{3+} or Hg^{2+} ions. The increase
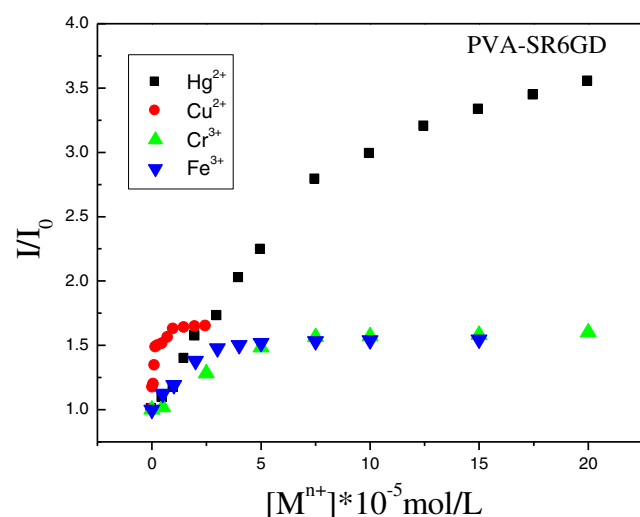
Fig. 5 The effects of Cu^{2+}, Fe^{3+}, Cr^{3+} or Hg^{2+} ions concentration ($[Cu^{2+}]$, $[Fe^{3+}]$, $[Cr^{3+}]$ or $[Hg^{2+}]$) on relative fluorescence intensity (I/I_0) of PVA-SR6GH (Cp=1.0 mg/mL; λex=500 nm; $[M^{n+}]$ was $[Cu^{2+}]$, $[Fe^{3+}]$, $[Cr^{3+}]$, or $[Hg^{2+}]$)

of the fluorescence intensity occured after the addition of Cu^{2+}, Fe^{3+}, Cr^{3+} or Hg^{2+} ions in the concentration range from Cu^{2+}, Fe^{3+}, Cr^{3+} or Hg^{2+}-free solution to 2.0×10^{-3}, 1.5×10^{-4}, 2.0×10^{-4} or 4.0×10^{-4} mol/L, respectively. The fluorescence intensity value remained constant above certain concentration. The relative fluorescence intensity enhanced nearly 1.64, 1.55, 1.60, or 4.14 times, respectively. However, we attempted addition of Cu^{2+}, Fe^{3+}, Cr^{3+} or Hg^{2+} ions to aqueous solution of the PVA-SR6GH and did not find any significant changes in the relative fluorescence intensity [18, 22, 31, 44, 45].

Figure S12 showed the comparative response of PVA-SR6GH to Cu^{2+}, Fe^{3+}, Cr^{3+} or Hg^{2+} in aqueous solution. The dependence of the relative fluorescence intensity (I/I_0) versus the concentration of Cu^{2+}, Fe^{3+}, Cr^{3+} or Hg^{2+} ($[M^{n+}]$) in the certain concentration range (0 to 2.0×10^{-4}, 0 to 3.0× 10^{-5}, 0 to 5.0×10^{-5} or 0 to 7.5×10^{-5} mol/L) exhibited quite good linear correlation, which were described by Eqs. 4–7 with the correlation coefficient 0.9827, 0.9906, 0.9929 or 0.9968, respectively [31, 45, 46].

$$I/I_0 = 1.0098 + 2.269 \times 10^3 \left[Cu^{2+}\right] \qquad (4)$$

$$I/I_0 = 1.0281 + 1.5908 \times 10^4 \left[Fe^{3+}\right] \qquad (5)$$

$$I/I_0 = 0.9944 + 1.0094 \times 10^4 \left[Cr^{3+}\right] \qquad (6)$$

$$I/I_0 = 1.0014 + 2.4423 \times 10^4 \left[Hg^{2+}\right] \qquad (7)$$

The detection limits for Cu^{2+}, Fe^{3+}, Cr^{3+} and Hg^{2+}ions in the same medium were found to be 6.61×10^{-11}, 7.51×10^{-11}, 4.45×10^{-11} and 1.23×10^{-12} mol/L [18, 23, 31, 42].

As mentioned previously, the color reaction of PVA-MRBH with Cu^{2+} or Fe^{3+} were attributed to the ring-opening of the spirolactam structure promoted by Cu^{2+} or Fe^{3+} complexation. However, the reaction system showed fluorescence quenching, which was rather different from that of the common rhodamine spirolactam derivatives [12, 13, 17] and PVA-SR6GH. Sun et al. [3] have investigated this unusual reaction mechanism by a comparative study on N-mono-maleic acid amide-N′-rhodamine B hydrazide (MRBH) and model compound N-acryloyl rhodamine B hydrazide (ARB). They believd that the extra carboxyl group in CARB played a crucial role in the color-on reaction, and without it the reaction

Fig. 6 Fluorescence response of PVA-MRBH (8.5 mg/mL) to 2.50×10^{-4} mol/L of Cu^{2+} or Fe^{3+} and other metal ions (the *red bar* portion) and to the mixture of 2.50×10^{-4} mol/L of other metal ions with 2.50×10^{-4} mol/L Cu^{2+} (the *green bar* portion) or Fe^{3+} (the *blue bar* portion)
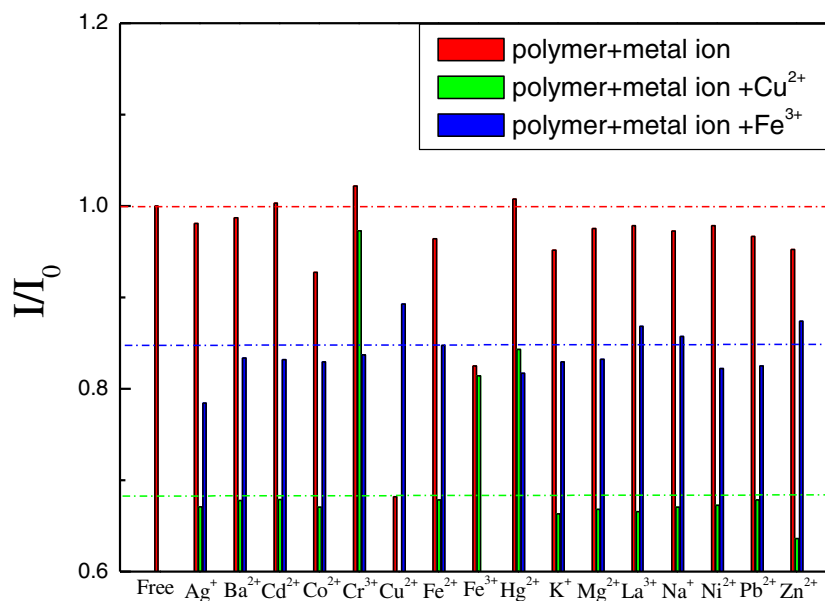
could not occur. According to MRBH and Cu^{2+} been formed complex with 1:2 stoichiometry, they conjectured that the two Cu^{2+} ions in the complex may play different roles: one induces the opening of the spirocyclic structure and the other quenches the fluorescence of the xanthene moiety. We further found that it is the single and double bonds in linkers that affects the sensing mode. It's derivatives can be enhanced for the former and quenching for the latter by metal ions.

Selectivity and Competitiveness of PVA-MRBH and PVA-SR6GH

Relative fluorescence intensity has been used as a quantitative measure of the effects of metal cations (including in Ag^+, Ba^{2+}, Cd^{2+}, Co^{2+}, Cr^{3+}, Cu^{2+}, Fe^{2+}, Fe^{3+}, Hg^{2+}, K^+, La^{3+}, Mg^{2+}, Na^+, Ni^{2+}, Pb^{2+}, and Zn^{2+} cations, metal cations concentration was 2.50×10^{-4} mol/L, polymer concentration was 8.5 and 1.0 mg/mL for PVA-MRBH and PVA-SR6GH) on relative fluorescence intensity [30]. The changes in the relative fluorescence intensity (I/I_0) of PVA-MRBH and PVA-SR6GH induced by the metal cations were investigated and presented in Figs. 6 and 7. As seen from Fig. 6, the addition of metal cations led to a decrease or increase of the fluorescence intensity for the polymer system, which was different for each metal cation. The PVA-MRBH has no response for fluorescence spectra upon the addition of Cd^{2+}. There were small fluorescence enhancement for Cr^{3+} and Hg^{2+}. The fluorescence quenching effects were observed in the presence of most of these metal cations, but the highest for Cu^{2+}, then the Fe^{3+} ions. As seen from Fig. 7, there were small changes of fluorescence intensity for PVA-SR6GH adding Ag^+, Ba^{2+}, Cd^{2+}, Co^{2+}, Fe^{2+}, K^+, La^{3+}, Mg^{2+}, Na^+, Ni^{2+}, Pb^{2+}, and Zn^{2+} cations, but there were highest fluorescence enhancement for PVA-SR6GH upon addition of Cu^{2+}, Fe^{3+}, Cr^{3+} and Hg^{2+} [30, 31, 44, 46, 47].

The competitive experiments were conducted by adding Cu^{2+} or Fe^{3+} ions (2.5×10^{-4} mol/L) to the solution of PVA-MRBH ($Cp=8.5$ mg/mL) in the presence of 2.5×10^{-4} mol/L of other metal ions (Ag^+, Ba^{2+}, Cd^{2+}, Co^{2+}, Cr^{3+}, Fe^{2+}, Hg^{2+}, K^+, La^{3+}, Mg^{2+}, Na^+, Ni^{2+}, Pb^{2+} and Zn^{2+}, see Fig. 6). The results further revealed that for PVA-MRBH, other metal ions, except for Cr^{3+}, Hg^{2+}, Fe^{3+} and Zn^{2+} ions, did not interfere with Cu^{2+}-induced fluorescence quenching. Ag^+, Cu^{2+}, La^{3+}, and Zn^{2+} ions can slightly interfere with the fluorescence quenching of PVA-MRBH moieties by Fe^{3+} ions.

The competitive experiments were also carried out by adding Cu^{2+}, Fe^{3+}, Cr^{3+} or Hg^{2+} ions (5.0×10^{-5} mol/L) to the solution of PVA-SR6GH ($Cp=1.0$ mg/mL) in the presence of 5.0×10^{-4} mol/L of other metal ions (Ag^+, Ba^{2+}, Cd^{2+}, Co^{2+}, Fe^{2+}, K^+, La^{3+}, Mg^{2+}, Na^+, Ni^{2+}, Pb^{2+} and Zn^{2+}) as shown in Fig. 7. As shown in Fig. 7a, most cations, such as Ag^+, Co^{2+}, K^+ and Pb^{2+}, had negligible influence on Cr^{3+}. However, Fe^{3+} ion led to a significant fluorescence enhancement for the solution of the PVA-SR6GH and Cr^{3+}, while the Cu^{2+} ion led to a significant fluorescence quenching of the solution of the PVA-SR6GH and Cr^{3+}. From Fig. 7a, it also can be seen that among a series of cations in PVA-SR6GH aqueous solution, including Ag^+, Ba^{2+}, Cd^{2+}, Co^{2+}, Cr^{3+}, Cu^{2+}, Fe^{2+}, Fe^{3+}, Hg^{2+}, K^+, La^{3+}, Mg^{2+}, Na^+, Ni^{2+}, Pb^{2+}, and Zn^{2+} cations, adding of Cu^{2+}, only Hg^{2+} made a considerable fluorescence enhancement, which interfered with Cu^{2+}-induced fluorescence enhancement. As shown in Fig. 7b, the Fe^{3+}-induced luminescence enhancement was not obviously affected in the presence of environmentally relevant alkali, alkaline-earth metals as well as other cations mentioned above, except for Hg^{2+}, $Cu^{2+}$and Fe^{2+}. It could also be seen from Fig. 7b that besides Ag^+, Cu^{2+}, Fe^{2+} and Fe^{3+}, other ions all had not seriously interfered on Hg^{2+} [22, 31, 47].

Fig. 7 Fluorescence response of PVA-SR6GH (1.0 mg/mL) to 5.0×10^{-4} mol/L of Cu^{2+}, Fe^{3+}, Cr^{3+} or Hg^{2+} and other metal ions (the *red bar* portion) and to the mixture of 5.0×10^{-4} mol/L of other metal ions with 5.0×10^{-4} mol/L Cu^{2+} (the *blue bar* portion), Fe^{3+} (the *cyan bar* portion) Cr^{3+} (the *green bar* portion) or Hg^{2+} (the *magenta bar* portion)
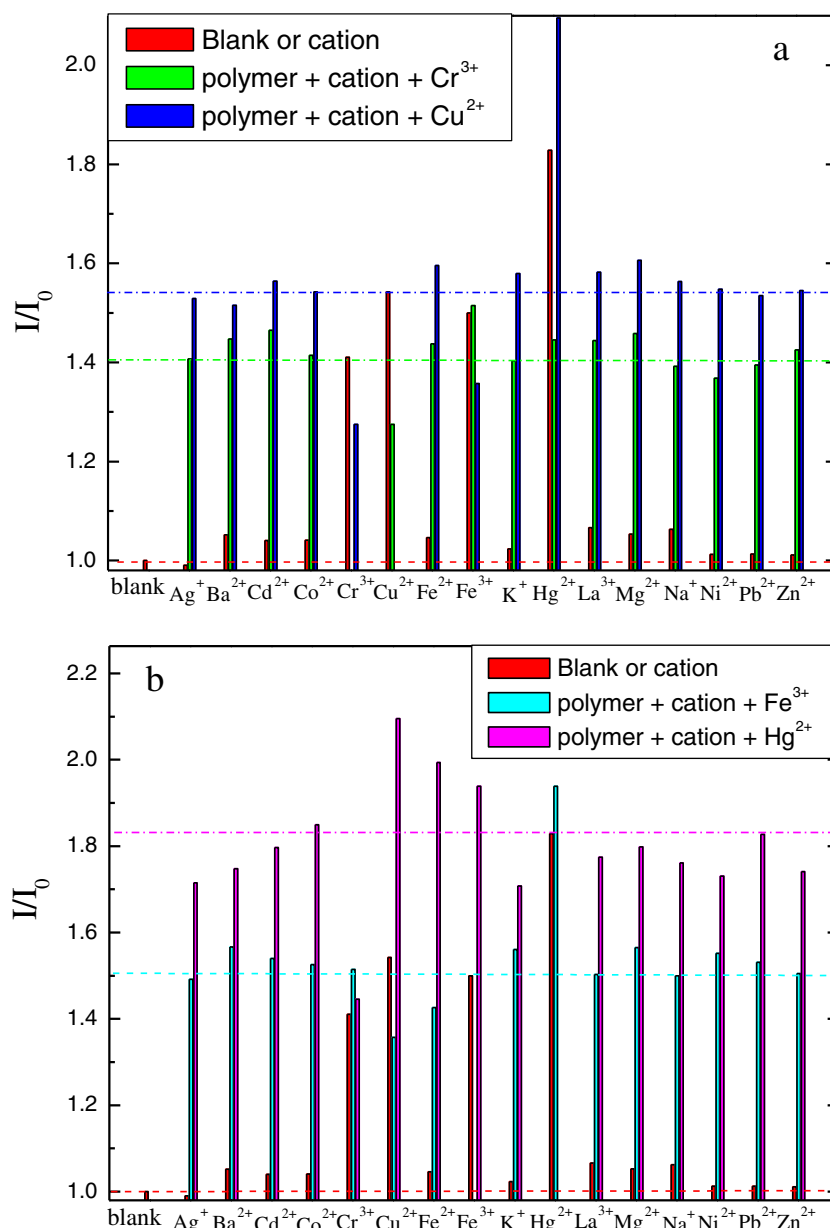

The color and fuorescence changes of PVA-MRBH (Cp=8.5 mg/mL) or PVA-SR6GH (Cp=1.0 mg/mL) up-on the addition of various cations (Ag^+, Ba^{2+}, Cd^{2+}, Co^{2+}, Cr^{3+}, Cu^{2+}, Fe^{2+}, Fe^{3+}, Hg^{2+}, K^+, La^{3+}, Mg^{2+}, Na^+, Ni^{2+}, Pb^{2+} and Zn^{2+}, 2.50×10^{-4} mol/L) are shown in Fig. 8. Figure 8 (Top (a), under visible light) showed that when Cu^{2+} or Fe^{3+} ions were added into the aque-ous solution of PVA-MRBH, the dramatic color of the solution changes occured from slight pink to magenta or orange red, respectively. Moreover, we also noted that the rate of chromogenic reaction for Cu^{2+} was faster than for Fe^{3+} ions. Under the same conditions, upon additions of other ions including Ag^+, Ba^{2+}, Cd^{2+}, Co^{2+}, Cr^{3+}, Fe^{2+}, Hg^{2+}, K^+, La^{3+}, Mg^{2+}, Na^+, Ni^{2+},

Pb^{2+} and Zn^{2+} resulted in small or no obvious color changes. Under UV light at 365 nm (Fig. 8, Top (b)), the colors of the aqueous solution of PVA-MRBH were changed from weak yellow to dark upon the addition of Cu^{2+} or Fe^{3+} ions, which could be ascribed to the fluo-rescence quenching of PVA-MRBH by Cu^{2+} or Fe^{3+} ions.

Figure 8 (Bottom) showed that when the metal cat-ions mentioned above were added into the solution of PVA-SR6GH, the color changes of the solution occured from colorless to yellow for Fe^{3+}. Although Cr^{3+}, Cu^{2+} and Hg^{2+} could make fluorescence of PVA-SR6GH enhancing, there were no color changes while added these three cations [18, 21, 22, 31, 44, 46, 48].

Fig. 8 Images of color reactions of PVA-MRBH (8.50 mg/mL) and PVA-SR6GH (1.0 mg/mL) with various ions (Ag^+, Ba^{2+}, Cd^{2+}, Co^{2+}, Cr^{3+}, Cu^{2+}, Fe^{2+}, Fe^{3+}, Hg^{2+}, K^+, La^{3+}, Mg^{2+}, Na^+, Ni^{2+}, Pb^{2+}, and Zn^{2+} cations at the same concentration of 2.50×10^{-4} mol/L). Reactions were performed at room temperature for 10 min in aqueous solution. **a** under visible light; **b** UV light at 365 nm

Top: PVA-MRBH (8.5mg/mL)

Bottom: PVA-SR6GH (1.0 mg/mL)
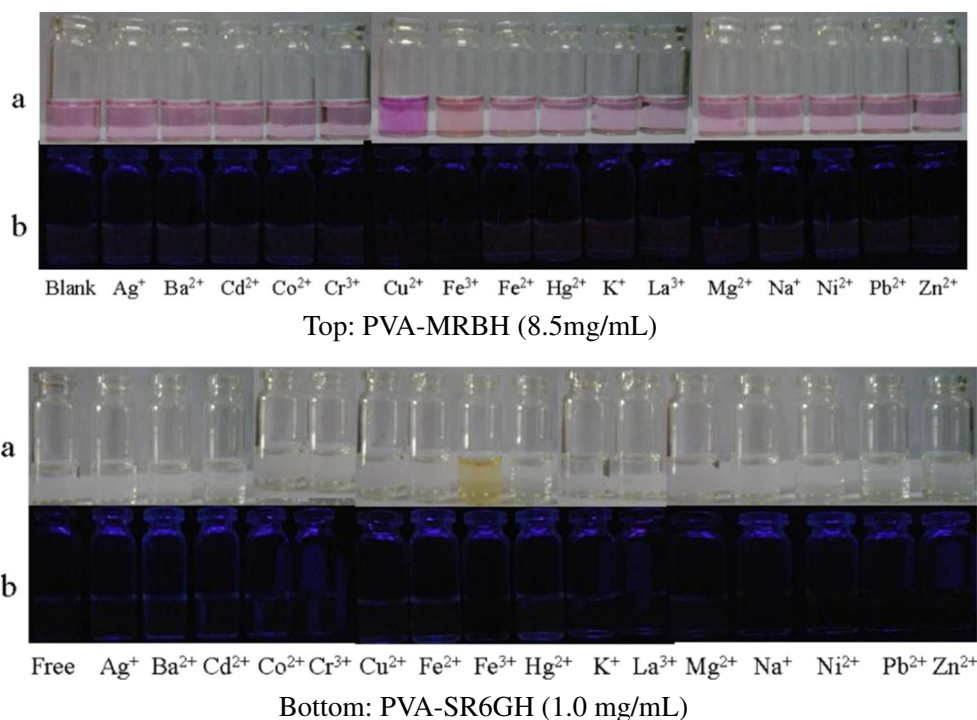
Conclusions

In summary, a simple and low-cost post-functionalization strategy was adopted to prepare two fluorescent polymeric chemosensors, PVA-MRBH and PVA-SR6GH, by covalent coupling of fluorescent molecular MRBH and SR6GH to water-soluble polyving akohols (PVA). It was found that although there were only a difference in single and double in the linkers, they possessed wholly diverse properties in fluorescent sensory pattern, metal cation species and color changes in aqueous solution. PVA-MRBH could sense Cu^{2+} and Fe^{3+} metal cations with fluorescence quenching pattern, while PVA-SR6GH could respond Cr^{3+}, Cu^{2+}, Fe^{3+} and Hg^{2+} metal cations with fluorescence enhancements. Moreover, PVA-MRBH and PVA-SR6GH had favorable colorimetric properties. When titration of Cu^{2+} and Fe^{3+} into PVA-MRBH, the change of clear color occured from rose pink to amaranth and orange, respectively. Upon the addition of Cr^{3+}, Cu^{2+}, Fe^{3+} and Hg^{2+} into the aqueous solution of PVA-SR6GH, only Fe^{3+} could make the color of the solution changing from colorless to yellow.

References

1. Li LQ, Meng LP (2014) Novel rhodamine derivate as high selective detection lead sensor. Spectrochim Acta A Mol Biomol Spectrosc 58: 772–775

2. Liu WY, Li HY, Lv HS, Zhao BX, Miao JY (2012) A rhodamine chromene-based turn-on fluorescence probe for selectively imaging Cu^{2+} in living cell. Spectrochim Acta A Mol Biomol Spectrosc 95: 658–663

3. Sun CD, Chen JM, Ma H, Liu Y, Zhang JH, Liu QJ (2011) A new Cu^{2+}-induced color reaction of a rhodamine derivative N-(3-carboxy)acryloyl rhodamine B hydrazide. Sci China Chem 54(7): 1101–1108

4. Kumari N, Dey N, Bhattacharya S (2014) Remarkable role of positional isomers in the design of sensors for the ratiometric detection of copper and mercury ions in water. RSC Adv 9:4230–4238

5. Karthigeyan DMD, Kundu TK, Govindaraju T (2013) FRET-based rational strategy for ratiometric detection of Cu^{2+} and live cell imaging. Sensors Actuator B Chem 176:831–837

6. Fang XX, Zhang SF, Zhao GY, Zhang WW, Xu JW, Ren AM, Wu CQ, Yang W (2014) The solvent-dependent binding modes of a rhodamine-azacrown based fluorescent probe for Al^{3+} and Fe^{3+}. Dyes Pigments 101:58–66

7. Chereddy NR, Suman K, Korrapati PS, Thennarasu S, Mandal AB (2012) Design and synthesis of rhodamine based chemosensors for the detection of Fe^{3+} ions. Dyes Pigments 95:606–613

8. Chai MM, Zhang D, Wang M, Hong HJ, Ye Y, Zhao YF (2012) Four rhodamine B-based fluorescent chemosensor for Fe^{3+} in aqueous solution. Sensors Actuators B Chem 174:231–236

9. Wang BY, Guan XL, Hu YL, Su ZX (2008) Synthesis and photophysical behavior of a water-soluble fluorescein-bearing polymer for Fe^{3+} ion sensing. J Polym Res 15:427–433

10. Ju HY, Lee MH, Kim J, Kim JS, Kim J (2011) Rhodamine-based chemosensing monolayers on glass as a facile fluorescent "turn-on" sensing film for selective detection of Pb^{2+}. Talanta 83:1359–1363

11. Wan XX, Liu HY, Yao S, Liu TQ, Yao YW (2014) A Stimuli-responsive nanogel-based sensitive and selective fluorescent sensor for Cr^{3+} with thermo-induced tunable detection sensitivity. Macromol Rapid Commun 35:323–329

12. Kim HN, Lee MH, Kim HJ (2008) A new trend in rhodamine-based chemosensors: application of spirolactam ring-opening to sensing ions. Chem Soc Rev 37:1465–1472

13. Bejia M, Afonso CAM, Martinho JMG (2009) Synthesis and applications of rhodamine derivatives as fluorescent probes. Chem Soc Rev 8:2410–2433

14. Chen X, Wang X, Wang S, Shi W, Wang K, Ma H (2008) A highly selective and sensitive fluorescence probe for the hypochlorite. Chem Eur J 14:4719–4724

15. Boyarskiy VP, Belov VN, Medda R, Hell SW (2008) Photostable, amino reactive and water-soluble fluorescent labels based on sulfonated rhodamine with a rigidized xanthene fragment. Chem Eur J 14:1784–1792

16. Dujols V, Ford F, Czarnik AW (1997) A long-wavelength fluorescent chemodosimeter selective for Cu (II) ion in water. J Am Chem Soc 119:7386–7387

17. Chen X, Pradhan T, Wang F, Kim JS, Yoon J (2012) Fluorescent chemosensors based on spiroring-opening of xanthenes and related derivatives. Chem Rev 112:1910–1956

18. Hamid EK, Pedro E, Saturnino I, Félix CG, Felipe S, Fouad BB, José MG (2013) Chromogenic and fluorogenic detection of cations in aqueous media by means of an acrylic polymer chemosensor with pendant rhodamine-based dyes. Dyes Pigments 96:414–423

19. Liu YH, Meng LZ, Lu XJ, Zhang LF, He YB (2008) Thermo and pH sensitive fluorescent polymer sensor for metal cations in aqueous solution. Polym Adv Technol 19:137–143

20. Wanichacheva N, Praikaew P, Suwanich T, Sukrat K (2014) "Naked-eye" colorimetric and "turn-on" fluorometric chemosensors for reversible Hg(2+) detection. Spectrochim Acta A Mol Biomol Spectrosc 118:908–914

21. Liu T, Liu SY (2011) Responsive polymers-based dual fluorescent chemosensors for Zn^{2+} ions and temperatures working in purely aqueous media. Anal Chem 8:32775–32785

22. Niamsa N, Kaewtong C, Srinonmuang W, Wanno B, Pulpokab B, Tuntulani T (2013) Hybrid organic–inorganic nanomaterial sensors for selective detection of Au^{3+} using rhodamine-based modified polyacrylic acid (PAA)-coated FeNPs. Polym Chem 4:3039–3046

23. Lee SH, Parthasarathy A, Schanze KS (2013) A sensitive and selective mercury (II) sensor based on amplified fluorescence quenching in a conjugated polyelectrolyte/spiro-cyclic rhodamine system. Macromol Rapid Commun 34:791–795

24. Geng TM, Wang Y, Huang RY (2014) Fluorescence sensors for selective detection of Hg^{2+} ion using a water-soluble poly(vinyl alcohol) bearing rhodamine B moieties. J Fluoresc 24:1207–1213

25. Geng TM, Wu DY, Huang W, Huang RY, Wu GH (2014) Fluorogenic detection of Hg^{2+}, Cd^{2+}, Fe^{2+}, Pb^{2+} cations in aqueous media by means of an acrylamide-acrylic acid copolymer chemosensor with pendant rhodamine-based dyes. J Polym Res: 21354–21361

26. Geng TM, Huang RY, Wu DY (2014) Turn-on fluorogenic and chromogenic detection of Fe^{3+} and Cr^{3+} in a completely water medium with polyacrylamide covalently bonding to rhodamine B using diethylenetriamine as a linker. RSC Adv 4(86):46332–46339

27. Fan JC, Chen J, Yang LM, Lin H, Cao FQ (2009) Preparation of dual-sensitive graft copolymer hydrogel based on N-maleoyl-chitosan and poly(N-isopropylacrylamide) by electron beam radiation. Bull Mater Sci 32:521–526

28. Yu YQ, Li YS, Liu LX, Zhu CJ, Xu Y (2011) Synthesis and characterization of pH and thermoresponsive Poly(N-isopropylacrylamideco-itaconic acid) hydrogels crosslinked with N-maleyl chitosan. J Polym Res 18:283–291

29. Yan FY, Cao DL, Wang M, Yang N, Yu QH, Dai LF, Chen L (2012) A new rhodamine-based "Off-On" fluorescent chemosensor for Hg (II) ion and its application in imaging Hg (II) in living cells. J Fluoresc 22:1249–1256

30. Wang BY, Guan XL, Hu YL, Su ZX (2007) Y Preparation and fluorescent properties of poly(vinyl alcohol) bearing coumarin. Polym Adv Technol 18:529–534

31. Luo J, Jiang SS, Qin SH, Wu HQ, Wang Y, Jiang JQ, Liu XY (2011) Highly sensitive and selective turn-on fluorescent chemosensor for Hg^{2+} in pure water based on a rhodamine containing water-soluble copolymer. Sensors Actuators B Chem 160:1191–1197

32. Yang XF, Guo XQ, Zhao YB (2002) Development of a novel rhodamine-type fluorescent probe to determine peroxynitrite. Talanta 57:883–890

33. Xiang Y, Tong AJ, Jin PY, Ju Y (2006) New fluorescent rhodamine hydrazone chemosensor for Cu (II) with high selectivity and sensitivity. Org Lett 8:2863–2866

34. Huang W, Song CX, He C, Lv GJ, Hu XY, Zhu X, Duan CY (2009) Recognition preference of rhodamine-thiospirolactams for mercury (II) in aqueous solution. Inorg Chem 48:5061–5072

35. Yang YK, Yook KJ, Tae J (2005) A rhodamine-based fluorescent and colorimetric chemodosimeter for the rapid detection of Hg^{2+} ions in aqueous media. J Am Chem Soc 127:16760–16761

36. Dong ZP, Yang B, Jin J, Li J, Kang HW, Zhong X, Ri L, Ma JT (2009) Quinoline group modified carbon nanotubes for the detection of zinc ions. Nanoscale Res Lett 4:335–340

37. Hu QM, Huang GS, Zheng J, Su H, Guo C (2012) Synthesis and rheological properties of hydrophobically modified poly(vinyl alcohol). J Polym Res 19:1–9

38. Kumar KS, Ramakrishnappa T, Balakrishna RG, Pandurangappa M (2014) A fluorescent chemodosimeter for Hg^{2+} based on a spirolactam ring-opening strategy and its application towards mercury determination in aqueous and cellular media. J Fluoresc 24:67–74

39. Kempahanumakkagaari SK, Thippeswamy R, Malingappa P (2014) A new rhodamine B based fluorometric chemodosimeter for Cu^{2+} ion in aqueous and cellular media. J Lumin 146:11–17

40. Zhang D, Li M, Wang M, Wang JH, Yang X, Ye Y, Zhao YF (2013) A rhodamine-phosphonate off–on fluorescent sensor for Hg^{2+} in natural water and its application in live cell imaging. Sensors Actuators B Chem 177:997–1002

41. Wang M, Yan FY, Zou Y, Chen L, Yang N, Zhou XG (2014) Recognition of Cu^{2+} and Hg^{2+} in physiological conditions by a new rhodamine based dual channel fluorescent probe. Sensors Actuators B Chem 192:512–521

42. Kim KN, Choi MG, Noh JH, Ahn S, Chang SK (2008) Rhodamine B hydrazide revisited: chemodosimetric Hg^{2+}-selective signaling behavior in aqueous environments. Bull Korean Chem Soc 29:571–574

43. He L, So VLL, Xin JH (2014) A new rhodamine-thiourea/Al^{3+} complex sensor for the fast visual detection of arginine in aqueous media. Sensors Actuators B Chem 192:496–502

44. Yuan L, Lin WY, Xie YN, Chen B, Zhu SS (2012) Single fluorescent probe responds to H_2O_2, NO, and H_2O_2/NO with three different sets of fluorescence signals. J Am Chem Soc 134:1305–1315

45. Popescu I, Airinei A, Suflet DM, Popa MI (2011) Maleic acid–2–vinylna phthalene copolymer in aqueous solution: investiga tion of the dissociation and fluorescence quenching. J Polym Res 18:2195–2203

46. Kaya İ, Kamacı M (2013) Highly selective and stable florescent sensor for Cd(II) based on poly(azomethine-urethane). J Fluoresc 23:115–121

47. Gao W, Yang YT, Huo FJ, Yin CX, Xu M, Zhang YB, Chao JB, Jin S, Zhang SP (2014) An ICT colorimetric chemosensor and a non-ICT fluorescent chemosensor for the detection copper ion. Sensors Actuators B Chem 193:294–300

48. Hu ZQ, Du M, Zhang LF, Guo FY, Liu MD, Li M (2014) A novel colorimetric and fluorescent chemosensor for cyanide ion in aqueous media based on a rhodamine derivative in the presence of Fe^{3+} ion. Sensors Actuators B Chem 193:439–443